

Computed Tomographic Imaging of Rabbit Bulbourethral Glands

R. Dimitrov

Department of Veterinary Anatomy, Histology and Embryology,
Faculty of Veterinary Medicine, Trakia University, 6000 Stara Zagora, Bulgaria

Abstract: Rabbit bulbourethral glands are a compact structure, surrounded by the skeletal M. bulboglandularis and a fibrous capsule. The glands have a cubic shape and are located on the dorsal urethral wall in craniocaudal direction. It is connected with prostate and paraprostate by a connective tissue. Ten sexually mature healthy male white New Zealand rabbits, 12 months old weighed 2.8-3.2 kg were investigated. The animals were anesthetized with 15 mg kg⁻¹ Zoletil® 50. Scans were done at 2 mm intervals and the image reconstruction was three-dimensional. The cuts were cranially limited between the body of the ischium behind the acetabulum (laterally) and the end of the ischial part of pubic symphysis (ventrally) and the first coccygeal vertebrae (cg1) (dorsally) and caudally-from the body of ischium, cranially to tuber ischiadicum (laterally), the ischial arch (ventrally) and the edge of the second coccygeal vertebrae (cg2). Rabbit bulbourethral glands were observed as a transversely oval homogeneous, relatively hyperdense structure against the surrounding soft tissues. They are visualized in the transverse cut of the pelvic outlet in the plane through the cranial part of cg2 (dorsally), the body of ischium, cranially to tuber ischiadicum (laterally) and dorsally to the caudal part of symphysis pubis-sciatic arch. The glandular margins are adequately distinguished from the adjacent soft tissue structures. The density of the rabbit bulbourethral glands was similar to this of the soft tissues (34±0.53 HU in native scan and up to 60±91 HU in contrast-enhanced scan). The width of the glands (lateral dimension) was 6.1±0.29 mm, its height (dorsoventral dimension) was 5.4±0.22 mm and the length (craniocaudal dimension) was 7.8±0.38 mm. The data obtained by the computed tomographic imaging of the rabbit bulbourethral glands could be used as an anatomical reference in the diagnosis and interpretation of imaging findings of various pathological states of the gland in this species, as well as in utilization of the rabbit as an animal model for studying diseases of this organ in humans, particularly diverticula, stenosis, lithiasis and valves.

Key words: Bulbourethral glands, computer tomography, rabbit, diagnosis, utilization, stenosis

INTRODUCTION

Rabbit bulbourethral glands are a compact structure, surrounded by the skeletal M. bulboglandularis and a fibrous capsule. The glands have a cubic shape and are located on the dorsal urethral wall in craniocaudal direction. They have short excretory ducts that drain on the caudodorsal wall of the bulbar urethra. The bulbourethral glands in rabbits are connected with prostate and paraprostate parts of the prostate gland via connective tissue (Vasquez and Del Sol, 2001; McCracken *et al.*, 2008). The bulbourethral glands are located in the connective tissue of the urogenital part of the perineum. Caudally, the glands are separated from the bulb of penis by the external fascia of the urogenital diaphragm (Barone, 1976).

In wild rodents, the glands are reported to be similar to these in domestic rodents (Mollineau *et al.*, 2006). The reproductive biology of the rodents (Mongolian gerbil) is connected directly with the development of the accessory sex glands and the way of their draining in the pelvic

urethra. The bulbourethral glands excrete in the pelvic urethra and their morphology is similar to these of the rats and mice (Pinheiro *et al.*, 2003). In the anatolu squirrel, the glands demonstrate a structure, similar to the glandular morphology in the domestic rabbit (Cakir and Karatas, 2004).

By computed tomography, the bulbourethral glands of the cats appeared as oval, soft-tissue, homogeneous and relatively hyperdense structures against the adjacent soft tissues. They were observed in transverse CT scans of the pelvic outlet between the third and fourth coccygeal vertebrae (dorsally), the sciatic arch (laterally) and caudodorsally to the caudal part of the symphysis pubis (Dimitrov and Toneva, 2005).

In men the bulbourethral glands are small, ovoid, yellowish, pea-sized structures. They are situated dorsolaterally, at the end of the membranous urethra, between the both fascias of the pelvic diaphragm. Depending on their localization, they are classified as diaphragmal, diaphragm-bulbar and bulbar. They release mucinous secretion, that drain in the beginning of

spongy urethra, prior to the ejaculation (Sikorski, 1977; Chughtai *et al.*, 2005). Imaging studies of the bulbourethral glands were performed by ultrasonography in stallions (Weber and Woods, 1993) and boars (Clark and Althouse, 2002). The bulbourethral glands in men were studied by intravenous voiding urography and they are small appendices of the male genital tract, visualized as duct opacities parallel to the urethra (Pedron *et al.*, 1997).

The pathologies affected bulbourethral glands in men are neoplasms, inflammations, lithiasis and cystic degeneration (syringocele) (Yaffe and Zissin, 1991). Bulbourethral cysts have been observed in the goat (Tarigan *et al.*, 1990) and the mouse (Wardrip *et al.*, 1998).

Radiologically, human bulbourethral glands were investigated to identify the relationship between the incidence of syringocele and urethral bulbar narrowing (Cobb's collar) (Dewan, 1996). The cystic degeneration of these glands in men has been explored by means of retrograde urethrography, computed tomography and magnetic resonance imaging (Cerqueira, 2004). The syringocele in men was observed by Kickuth *et al.* (2002) and Dombrovskii (2003) by computed and magnetic resonance tomography and the findings demonstrated homogeneous oval structures with cystic lesions, originating from the glands and compressing the bulbar urethra.

The scarce literature data about the anatomical imaging of domestic rabbits bulbourethral glands, especially computed tomography imaging, motivated the present investigations of the anatomical topographic traits of these glands in rabbits by means of axial computed tomography. The aim of the study was to utilize the obtained data for differentiation of normal and pathologically altered bulbourethral glands in rabbits with regard to using this animal species as a model for studying diseases in this organ in humans.

MATERIALS AND METHODS

Ten sexually matured, clinically healthy male white New Zealand rabbits, at age 12 months and weighed 2.8-3.2 kg were used in this study. The animals were anesthetized with 15 mg kg⁻¹ Zoletil® 50 (tiletamine hydrochloride 125 mg and zolazepam hydrochloride 125 mg in 5 mL of the solution) Virbac, France (Dinev and Simeonova, 2009).

The experiment was performed in compliance with the ethical guidelines for humane treatment of animals and European Communities Council Directive 86/609/EEC of 24 November 1986. The study was performed in strict compliance with the ethical guidelines for humane

treatment of animals as defined by the European convention for the protection of vertebrate animals used for experimental and other scientific purposes, the European Convention for the Protection of Pet Animals and Law on Animal Protection in the Republic of Bulgaria part IV (Animal Experimentation).

As contrast agents Optiray® 350 (ioversol 741 mg mL⁻¹), Healthcare Ltd., UK was applied intravenously at 1 mL kg⁻¹ in *V. cephalica* and the investigation was performed immediately. The second contrast medium was Urografin 76% (sodium amidotrizoate 0.1 g mL⁻¹ and meglumine amidotrizoate 0.66 g mL⁻¹), Schering Ltd., Germany, applied orally as a 1.52% aqueous solution (30 mL kg⁻¹, fractionated administration) and the imaging was performed 3 h later. An axial computer tomograph SIEMENS, SOMATOM, ARTX with table height 125 cm, FOV = 250, filter 1, anode current 70 mA, anode tension 110 kV, was used. The scanning time was 3 sec. A high-resolution 512 mode, gentry (GT)-0° was employed with Window (W)-280 and centre-53. Scans were done at intervals of 2 mm and image reconstruction was three-dimensional.

The cuts were cranially limited between the body of the ischium behind the acetabulum (laterally) and the end of the sciatic part of pubic symphysis (ventrally) and the first coccygeal vertebrae (cg1) (dorsally) and caudally from the body of the ischium cranially to tuber ischiadicum (laterally), the sciatic arch (ventrally) and the edge of the second coccygeal vertebrae (cg2).

About determination of the rabbit bulbourethral glands topography, the following bone markers were used: the respective vertebrae-dorsally, the pubic symphysis and the sciatic arch- ventrally and the body of ischium-laterally.

As soft tissue markers, the well-visualized native or contrast-enhanced bulbar urethra and native or contrast enhanced rectum were used. Five animals were positioned in ventral recumbency and the other 5 in dorsal recumbency. In two animals the CT imaging was native (without contrast amplification) in another four the contrast amplification was done with Optiray® 350 and in the last four with Urografin 76%. The transverse CT scans of the pelvis were performed in the transverse planes between the first and the second coccygeal vertebrae with cut thickness of 2 mm. The statistical processing of data was made by statistical software (StatMost for Windows, 1994).

RESULTS AND METHODS

The reconstructed image of the rabbit bulbourethral glands and the peripheral structures in dorsal and sagittal views were shown on Fig. 1 and Fig. 2. Bulbourethral glands were big homogeneous soft tissue findings, situated dorsolaterally against the contrast-enhanced

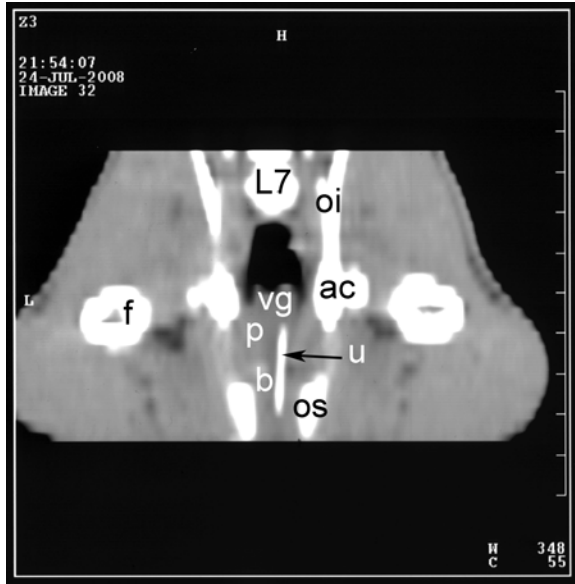


Fig. 1: Reconstructed CT image of accessory sexual glands and pelvic urethra in the rabbit (dorsal view)-vesicular glands (vg), prostatic complex (p), pelvic urethra (u), bulbourethral glands (b), body of ilium (oi), acetabulum (ac), ischium (os), seventh lumbar vertebrae (L7), femur (f)



Fig. 2: Reconstructed CT image of accessory sex glands and pelvic urethra in the rabbit (sagittal view)-vesicular glands (v), prostate complex (p), pelvic urethra (u), bulbourethral glands (b), seventh lumbar vertebrae (L7), pubis (op)

bulbar urethra. The glands were located behind the situated cranially prostate gland at the pelvic outlet. The

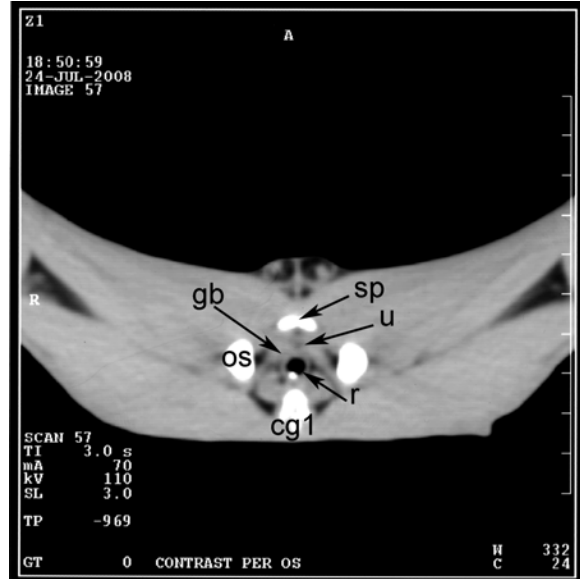


Fig. 3: Transverse CT image of rabbit pelvis through the first coccygeal vertebrae (cg1) (dorsal recumbency)-bulbar urethra (u), bulbourethral glands (gb), rectum (r), body of ischium (os), sciatic part of pubic symphysis (sp). Cut thickness 2 mm

transverse computer tomographic image of the pelvis through the first coccygeal vertebrae (Fig. 3) presents the caudal part of the sciatic part of pubic symphysis (ventromedially), the body of ischium (laterally) and the first coccygeal vertebra (dorsally). Dorsomedially to the caudal part of the symphysis rim, the native bulbar urethra was seen. Its lumen was hypodense whereas its wall-relatively hyperdense and homogeneous. Dorsally, beneath the rectum, the cranial parts of bulbourethral glands were visualized as soft-tissue relatively hyperdense structures against the urethral and rectal walls.

The results shown on Fig. 1-3 allowed us to assume that the initial appearance of a CT image of rabbit bulbourethral glands was in the transverse plane through the middle of the first coccygeal vertebrae, the body of ischium cranially to tuber ischiadicum and the caudal sciatic part of pubic symphysis.

The complete computed tomographic image of the rabbit bulbourethral glands was shown on Fig. 4 (cranial edge of cg2) where the lumen of the bulbar urethra was contrast-enhanced (hyperdense) and the glands were observed as hyperdense soft-tissue findings, located dorsolaterally to the urethra and under the ventral rectal wall at the pelvic outlet. Urethral and rectal walls were hypodense, compared to the glandular findings. Rabbit glands were transversely oval homogeneous relatively hyperdense structures as compared to the

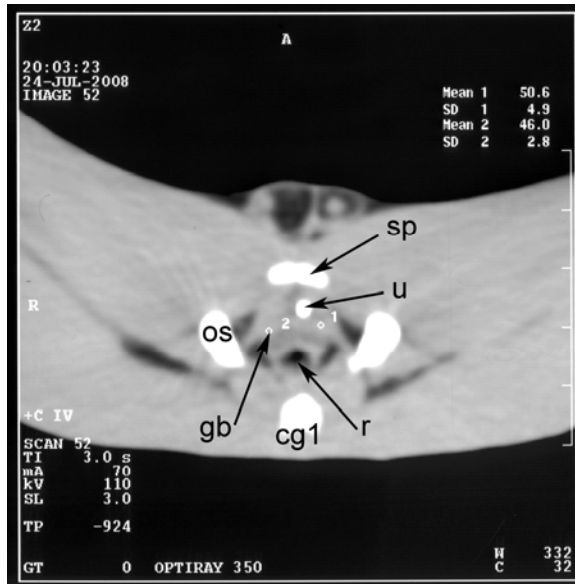


Fig. 4: Transverse CT image of rabbit pelvis through the cranial part of the second coccygeal vertebrae (cg2) (dorsal recumbency)-bulbar urethra (u), bulbourethral glands (gb), rectum (r), body of ischium (os), sciatic part of pubic symphysis (sp). Cut thickness 2 mm

adjacent soft tissues. They were observed in the transverse cut of the pelvic outlet in the plane through the cranial part of cg2 (dorsally), the body of ischium cranially to tuber ischiadicum (laterally) and dorsally to the caudal pubic symphysis-sciatic arch. The glandular margins were adequately distinguished from the adjacent soft tissue structures (Fig. 4).

CT image on the caudal end of cg2 (Fig. 5) presents the caudal parts of bulbourethral glands shown through the soft tissue findings over the contrast-enhanced bulbar urethra. The urethral lumen was hypodense and glandular areas-relatively hyperdense against the urethral and rectal walls. The caudal parts of the bulbourethral glands' images were observed on cuts of the pelvic outlet through the caudal part of the second coccygeal vertebrae, the body of ischium cranially to tuber ischiadicum and over the sciatic arch (Fig. 5).

The density of the rabbit bulbourethral glands was similar to that of the soft tissues (from 34 ± 0.53 HU-native to 60 ± 91 HU in contrast-enhanced image) (Fig. 4 and 5). The glands width (lateral size) was 6.1 ± 0.29 mm, its height (dorsoventral size) 5.4 ± 0.22 mm and its length (craniocaudal size) 7.8 ± 0.38 mm. The present computed tomographic imaging confirmed the findings obtained by native anatomical imaging techniques, that rabbit bulbourethral glands were in closed vicinity to the prostate gland. The dorsal surface of the membranous urethra

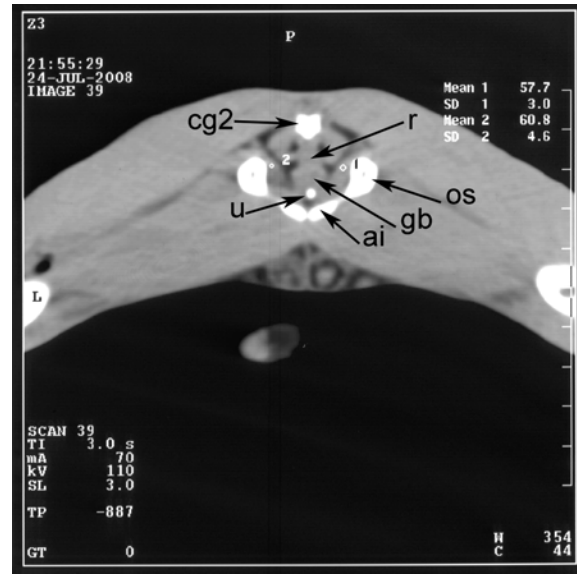


Fig. 5: Transverse CT image of rabbit pelvis through the caudal part of the second coccygeal vertebrae (cg2) (ventral recumbency)-bulbar urethra (u), bulbourethral glands (gb), rectum (r), sciatic arch (ai), body of ischium (os) Cut thickness 2 mm

was completely covered by the both glands (Barone, 1976; Vasquez and Del Sol, 2001; Holtz and Foote, 2005; Mollineau *et al.*, 2006; McCracken *et al.*, 2008).

The soft tissue characteristics of the rabbit bulbourethral glands and their structural features were similar to these of the cats (Dimitrov and Toneva, 2005). Unlike to feline bulbourethral glands, the rabbit ones were located relatively cranially and larger.

The size of the rabbit glands couldn't be compared to the human bulbourethral glands (Sikorski, 1977; Chughtai *et al.*, 2005) due to the small size of these glands in these animals. Rabbit bulbourethral glands showed a soft tissue density similar to this of the human glands (Cerqueira *et al.*, 2004; Dewan, 1996; Kickuth *et al.*, 2002). They appeared as homogeneous hyperdense findings like to the findings reported in men (Yaffe and Zissin, 1991; Pedron, 1997).

The localization and shape of the rabbit bulbourethral glands were different from these in men (pea-sized duct opacities parallel to the urethra parallel to the urethra) contrary to the studies of Kickuth *et al.* (2002), Dombrovskii (2003) and Chughtai *et al.* (2005).

In this study, three dimensions of the rabbit bulbourethral glands as this is made in the boar by Clark and Althouse (2002), the stallion by Weber and Woods (1993) and the goat presented by Tarigan *et al.* (1990). The rabbit bulbourethral glands and bulbar urethra

showed relatively similar imaging anatomical features as these in men, mouse and goat (Kickuth *et al.*, 2002; Dombrovskii, 2003; Wardrip *et al.*, 1998; Tarigan *et al.*, 1990). The computed tomography of the rabbit bulbourethral glands could assist in investigating their anatomical features and occurring abnormalities such as diverticula, stenosis, lithiasis and valves.

CONCLUSION

The data obtained from the present computed tomographic imaging study of the rabbit bulbourethral glands could be used as an anatomical source about the diagnosis and interpretation of imaging findings of various pathological states of the glands. The results could be useful in the utilization of the rabbit as an animal model for investigation of diseases in human bulbourethral glands.

REFERENCES

- Barone, R., 1976. Anatomie Comparee Des Mammiferes Domestiques. 2nd Edn., VIGOT., Paris.
- Cakir, M. and A. Karatas, 2004. Histo-anatomical studies on the accessory reproductive glands of the *Anatolian souslik* (*Spermophilus xantoprynus*) (Mammalia: Sciuridae). *Anatomia Histologia Embryol.*, 33: 146-150.
- Cerqueira, M., L. Xambre, V. Silva, R. Prisco and R. Santo *et al.*, 2004. Imperforate syringocele of the Cowper's glands laparoscopic treatment. *Actas Urol. Esp.*, 28: 535-538.
- Chughtai, B., A. Sawas, R. O'Malley, R. Naik, S. Alikhan and S. Pentyala, 2005. A neglected gland: A review of Cowper's gland. *Int. J. Androl.*, 28: 74-77.
- Clark, S. and G. Althouse, 2002. B-mode ultrasonographic examination of the accessory sex glands of boars. *Theriogenol.*, 57: 2003-2013.
- Dewan, P., 1996. A of the study relationship between syringoceles and Cobb's collar. *Eur. Urolol.*, 30: 119-124.
- Dimitrov, R. and Y. Toneva, 2005. Computed tomography features of *Bulbourethral glands* in the tomcat. *Trakia J. Sci.*, 3: 22-25.
- Dinev, D. and G. Simeonova, 2009. Veterinary Anaesthesiology. Kota Publishing House, Stara Zagora.
- Dombrovskii, V., 2003. Magnetic resonance tomography in the diagnosis of nonorganic bulky masses of the retroperitoneal space. Part 1. Cysts, abscesses and flegmons. *Vestnik Rentgenol. Radiol.*, 2: 48-60.
- Holtz, W. and R. Foote, 1978. The anatomy of the reproductive system in male Dutch rabbits (*Oryctolagus cuniculus*) with special emphasis on the accessory sex glands. *J. Morphol.*, 158: 1-20.
- Kickuth, R., U. Laufer, J. Pannek, T. Kirchner, E. Herbe and J. Kirchner, 2002. Cowper's syringocele: Diagnosis based on MRI findings. *Pediatr. Radiol.*, 32: 56-58.
- McCracken, T., R. Kainer and D. Carlson, 2008. Color Atlas of Small Animal Anatomy: The Essentials. Blackwell Publishing, USA., pp: 160.
- Mollineau, W., A. Adogwa, N. Jsaper, K. Young and G. Garcia, 2006. The gross anatomy of the male reproductive system of a neotropical rodent: The agouti (*Dasyprocta leprina*). *Anatomia Histol. Embryol.*, 35: 47-52.
- Pedron, P., O. Traxer, F. Haab, M. Farres, M. Tligui, P. Thibault and B. Gattegno, 1997. Cowper's gland: Anatomic, physiological and pathological aspects. *Prog. Urol.*, 7: 563-569.
- Pinheiro, P., C. Almeida, T. Segatelli, M. Martinez, C. Padovani and F. Martinez, 2003. Structure of the pelvic and penile urethra-relationship with the ducts of the sex accessory glands of the Mongolian gerbil (*Meriones unguiculatus*). *J. Anat.*, 202: 431-444.
- Sikorski, A., 1977. Macroscopic structure of the bulbourethral gland of man. *Arkh. Anat. Gistol. Embriol.*, 72: 27-31.
- StatMost for Windows, 1994. DataMost Corporation. StatMost Publisher, USA., pp: 87-96.
- Tarigan, S., P. Ladds and R. Foster, 1990. Genital pathology of feral male goats. *Aust. Vet. J.*, 67: 286-290.
- Vasquez, B. and M. Del Sol, 2001. Morphologic study of the bulbourethral gland of the rabbit (*Oryctolagus cuniculus*). *Rev. Chil. Anat.*, 19: 221-228 (Original Article in Spanish).
- Wardrip, C., J. Lohmiller, S. Swing, S. Seps and X. Li, 1998. Bulbourethral gland cysts in three mice. *Contemporary Topics in Lab. Anim. Sci.*, 37: 101-102.
- Weber, J. and G. Woods, 1993. Ultrasonographic measurement of stallion accessory sex glands and excurrent ducts during seminal emission and ejaculation. *Biol. Reprod.*, 49: 267-273.
- Yaffe, D. and R. Zissin, 1991. Cowper's glands duct: Radiographic findings. *Urol. Radiol.*, 13: 123-125.